Journal of Alloys and Compounds 480 (2009) 684–688

Contents lists available at ScienceDirect

Journal of Alloys and Compounds

journal homepage: www.elsevier.com/locate/jallcom

A facile microwave solvothermal process to synthesize $ZnWO_4$ nanoparticles

Jinhong Bi, Ling Wu*, Zhaohui Li, Zhengxin Ding, Xuxu Wang, Xianzhi Fu*

State Key Laboratory Breeding Base of Photocatalysis, Fuzhou University, Industry Road, Fuzhou 350002, PR China

ARTICLE INFO

Article history:
Received 30 October 2008
Received in revised form 3 February 2009
Accepted 7 February 2009
Available online 21 February 2009

Keywords:
Microwave
Solvothermal
Nanoparticles
$ZnWO_4$
Photocatalytic activity

ABSTRACT

$ZnWO_4$ nanoparticles were synthesized by a facile microwave-assisted solvothermal process. The X-ray diffraction results indicated that the as-synthesized nanoparticles exhibited only wolframite structure $ZnWO_4$ without impurities. The transmission electron microscopy (TEM) images revealed that the particle size of synthesized nanoparticles were around 10 nm. All samples showed a band-gap of 3.8 eV. The photocatalytic activities were evaluated by the decomposition of salicylic acid and Rhodamine B under UV light irradiations. The results showed that the samples prepared by the microwave solvothermal process exhibited higher photocatalytic activities than that prepared by the conventional solvothermal process.

1. Introduction

Metal tungstates with the formula of AWO_4 have attracted much interest since they can be used as scintillating medium and in electro-optic applications [1]. Depending on the ionic radius of the cation in A^{2+} sites, this family of compound can crystallize in either scheelite or wolframite structure. Tungstates with relatively large bivalent cations (ionic radius $\geq$0.99 Å: Ca, Ba, Pb, Sr) crystallize in the so-called scheelite structure (scheelite = $CaWO_4$), in which tungsten has a tetrahedral coordination. On the contrary, tungstates with smaller bivalent cations (ionic radius $\leq$0.77 Å: Fe, Mn, Co, Ni, Mg, Zn) crystallize in wolframite structure (wolframite = (Fe, Mn)WO_4), where tungsten exhibits an overall 6-fold coordination [2]. Among them, zinc tungstate ($ZnWO_4$) crystallizes in the wolframite structure. It has been known as an important scintillating, laser-host, photocatalyst and gas sensing material [3–7]. Up to now, various methods have been developed to synthesize nanocrystalline $ZnWO_4$, including Czochralski technique [8], sol–gel technique [9], hydrothermal processes [6,10], aqueous solution growth [11], polymerized complex method [12,13], hydrothermal combined with annealing treatment [14], template method [5], novel solid-state metathetic approach [15] self-propagating combustion method [16] and so on. Besides these established synthesis processes, finding simple and cost-effective routes to synthesize nanocrystalline $ZnWO_4$ is still a challenge.

Microwave irradiation has been applied for the rapid synthesis of inorganic solids and organic synthetic reactions [17]. As it causes internal heating of the material then lower temperatures and shorter times can be used compared to those applied on conventional heating [18]. It is an inexpensive, facile and fast method in preparing nanocrystalline samples with unique or enhanced properties. Besides this, several studies on the microwave-assisted synthesis of materials have revealed that the kinetics of the organic and inorganic chemical reactions can be accelerated significantly by microwave [19–21]. Therefore the utilization of microwave has been a focus. This process has been employed to synthesize various compounds such as $CaWO_4$, $SrWO_4$ [22], $BaWO_4$ [23], Bi_2WO_6 [24], hydroxyapatite nanostrips [25], $SrMoO_4$ [26], CdSe [27], ZnS:Mn^{2+} nanoparticles [28], ZnO [29], CeO_2 [30], Zn_2SiO_4 [31], $LaFeO_3$ [32], $BaMgAl_{10}O_{17}$:Eu^{2+} [33], Mg_2NiH_4 [34], Ni–Zn–Sm ferrites [35] and so on.

In the present study, we report the synthesis of nanocrystalline $ZnWO_4$ by a facile microwave solvothermal (MS) process for the first time. The synthesized nanocrystalline $ZnWO_4$ samples were characterized by X-ray diffraction (XRD) technique, Brunauer–Emmett–Teller (BET) surface measurements, transmission electron microscopy (TEM), UV–vis diffuse reflectance spectra (UV–vis DRS) and X-ray photoelectron spectroscopy (XPS). The photocatalytic activities of $ZnWO_4$ were investigated by the degradation of salicylic acid (SA) and Rhodamine B (RhB) under the irradiations of UV light (λ = 254 nm).

* Corresponding authors. Tel.: +86 591 83738608; fax: +86 591 83738608.
E-mail addresses: wuling@fzu.edu.cn (L. Wu), xzfu@fzu.edu.cn (X. Fu).

0925-8388/$ – see front matter © 2009 Elsevier B.V. All rights reserved.
doi:10.1016/j.jallcom.2009.02.029

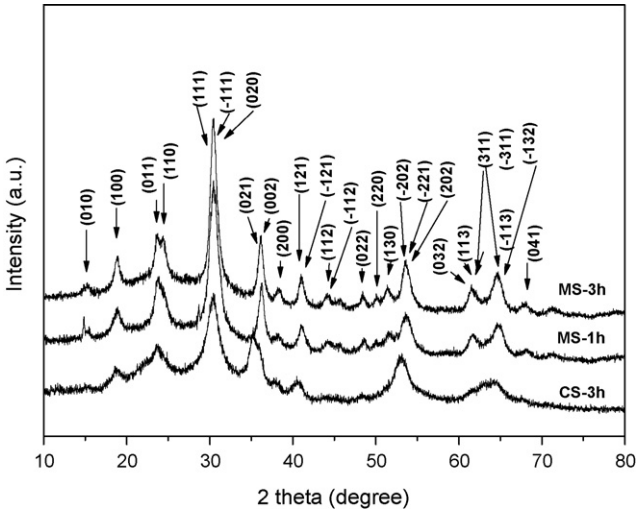

Fig. 1. XRD patterns of nanocrystalline $ZnWO_4$ samples prepared by microwave-solvothermal process (MS) and conventional solvothermal process (CS).

2. Experimental

2.1. Syntheses

$ZnSO_4{\cdot}7H_2O$, $5(NH_4)_2O{\cdot}12WO_3{\cdot}5H_2O$ and ethylene glycol were used as the starting materials. In a typical procedure, 1.3803 g of $ZnSO_4{\cdot}7H_2O$ and 1.2533 g of $5(NH_4)_2O{\cdot}12WO_3{\cdot}5H_2O$ were put into the Teflon lined digestion vessel. Then ethylene glycol was added. Under stirring 4 mol/L NaOH solution was added to adjust pH to 9. A vessel cover was used to seal the vessel and act as an overpressure release valve surrounded by a safety shield and then heated by a microwave synthesizer (ETHOS TC from Milestone Inc.) at 160 °C for different time. A white suspension formed after the microwave treatment. The products were washed by the deionized water and then dried at 80 °C before analysis. The samples obtained under 1 h and 3 h microwave irradiation are denoted as MS-1h and MS-3h, respectively. As a comparison, a conventional solvothermal process (CS, reaction temperature: 160 °C, reaction time: 3 h, pH = 9) was also conducted. The obtained $ZnWO_4$ sample was denoted as CS-3h.

2.2. Characterizations

The as-prepared samples were characterized by powder XRD on a Bruker D8 Advance X-ray diffractometer at 40 kV and 40 mA with Ni filtered Cu Kα radiation. Data were recorded at a scan rate of 0.02° $2\theta\,s^{-1}$ in the 2θ range 10–80°. The BET surface area was measured with ASAP2020M (Micromeritics Instrument Corp.). UV–vis diffuse reflectance spectra (UV–vis DRS) of the samples were obtained for the dry-pressed disk sample using a UV–vis spectrophotometer (Lambda-900, PerkinElmer). $BaSO_4$ was used as a reflectance standard. The TEM and the high resolution transmission electron microscopy (HRTEM) image was taken by JEOL model JEM 2010 EX instrument at the accelerating voltage of 200 kV. The powder particles were supported on a carbon film coated on a 3-mm diameter fine-mesh copper grid. A suspension in ethanol was sonicated, and a drop was dripped on the support film. XPS measurements were carried out by using a VG Scientific ESCA Lab 250 spectrometer where Twin anode X-Ray Gun Mg ka (E = 1253.6 eV) was used.

2.3. Photocatalytic activity test

Photocatalytic reactions were performed in a quartz tube with 4.7 cm in inner diameter and 16.5 cm in length. Four 4 W UV lamps with a wavelength centered at 254 nm (Philips, TUV4W/G4 T5) were used as illuminating source. One hundred milligrams of powdered photocatalysts were suspended in 150 mL of SA aqueous solution (2.5×10^{-4} mol/L) and RhB aqueous solution (10^{-5} mol/L). Before irradiation the suspension was stirred in the dark to ensure the reach of the adsorption/desorption equilibrium. A 3-mL aliquot was taken at 15 min intervals during the experiment and centrifuged. The resulting clear liquor was analyzed on a Varian Cary-50 UV–vis–NIR spectrophotometer. The percentage of degradation is reported

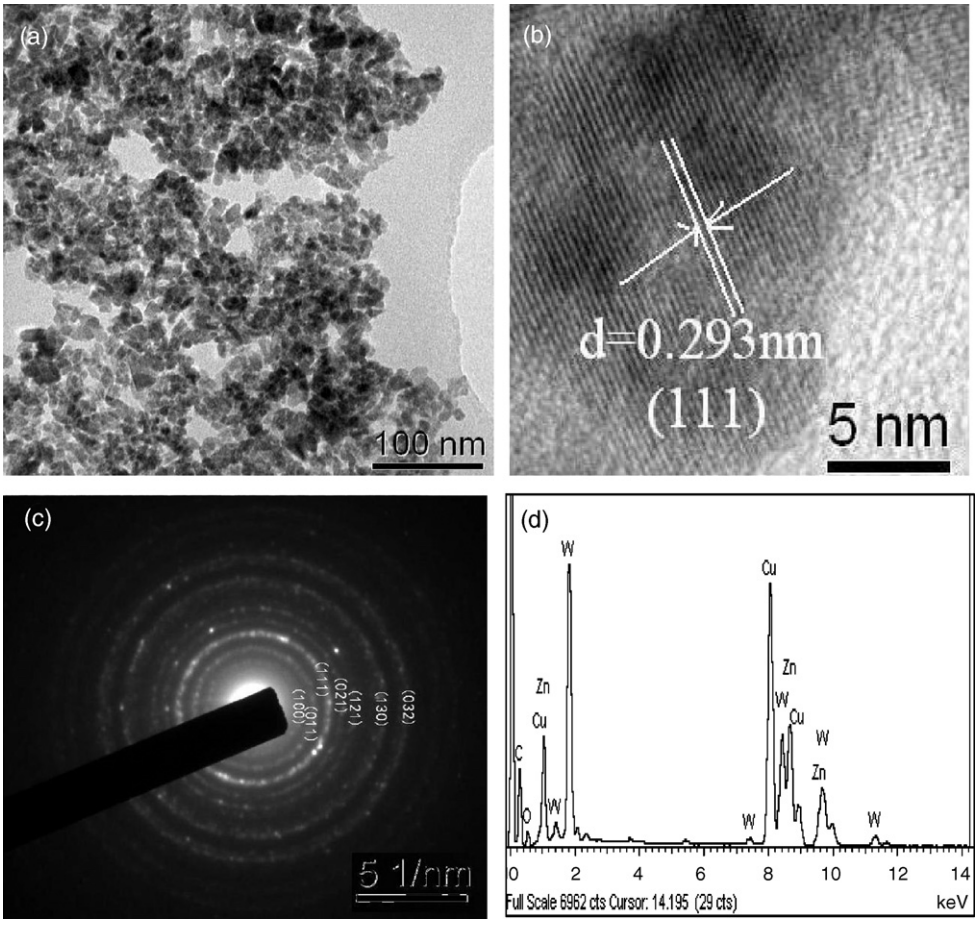

Fig. 2. TEM, HRTEM, SAED and EDS spectra of the sample prepared by the microwave solvothermal process for 3 h (MS-3h).

as C/C_0. C was the absorption of SA and RhB at each irradiated time interval of the main peak of the absorption spectrum at wavelength 297 nm and 554 nm, respectively. C_0 was the absorption of the starting concentration when adsorption/desorption equilibrium was achieved.

3. Results and discussion

The XRD patterns of the samples are shown in Fig. 1. All of the detected peaks are indexed to $ZnWO_4$ (JCPDS: 15-0774). No extra peaks are found. It is observed from the XRD patterns that with the increase of the treatment time, intensity of XRD peaks increased and full width at half maximum decreased, indicating the enhancement of the crystallinity and crystallite size. Compared with the conventional solvothermal route, the irradiation under the microwave produces a better crystallinity in a shorter treatment time. This indicates that the introduction of the microwave really can save energy and time with faster kinetics of crystallization [36–38]. The particle sizes were calculated from (1 1 1) peaks using Scherrer's formula $D = k\lambda/\beta\cos\theta$, where D is the average grain size, k a constant equal to 0.89, λ the wavelength of X-rays and β is the corrected half-width. The calculated average crystallite sizes of sample CS-3h, MS-1h and MS-3h are 6 nm, 7 nm and 9 nm, respectively. The BET specific surface areas for sample CS-1h, MS-1h and MS-3h are 69.4 m^2/g, 72.8 m^2/g and 70.3 m^2/g, respectively.

The morphology and structure of the powders were investigated by TEM and HRTEM. The TEM image (Fig. 2a) reveals that sample MS-3h shows uniform and dispersive particles with average particle size of around 10 nm, in agreement with the result calculated from Scherrer's formula in XRD. The HRTEM image (Fig. 2b) shows clear lattice fringes. The fringes of $d = 0.293$ nm match well with that of the (1 1 1) plane of $ZnWO_4$, which is the strongest crystallographic plane. The rings of selected area electron diffraction (SAED) (Fig. 2c) clearly show the diffraction of (0 3 2), (1 3 0), (1 2 1), (0 2 1), (1 1 1), (0 1 1) and (1 0 0) crystal planes, respectively from the outside to the inside of the ring. The EDS result (Fig. 2d) indicates that the sample contains Zn, W and O element.

The diffuse absorption coefficient $F(R)$ of $ZnWO_4$ nanoparticles is shown in Fig. 3. $ZnWO_4$ is an indirect-gap semiconductor. Depending on the Kubelka–Munk formula [39,40], the relationship between the absorption coefficient and the band-gap energy follows the formula: $(F(R)E)^{1/2} = A(E - E_g)$, in which E, E_g are photon energy and optical band-gap energy, respectively, and A is the characteristic constant of semiconductors. From the equation $(F(R)E)^{1/2}$ has a linear relation with E. Extrapolating the linear relation as $(F(R)E)^{1/2} = 0$ gives the band-gap E_g of approximately 3.8 eV as shown in Fig. 3 (inset).

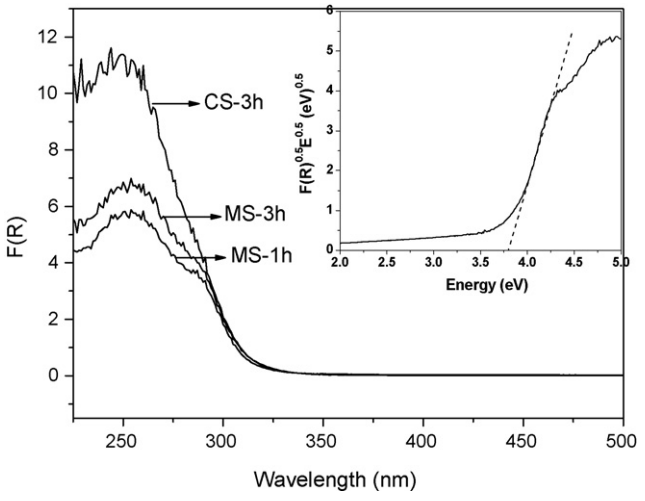

Fig. 3. UV–vis diffuse reflectance spectra of the samples: (inset) optical band-gap energy E_g of $ZnWO_4$.

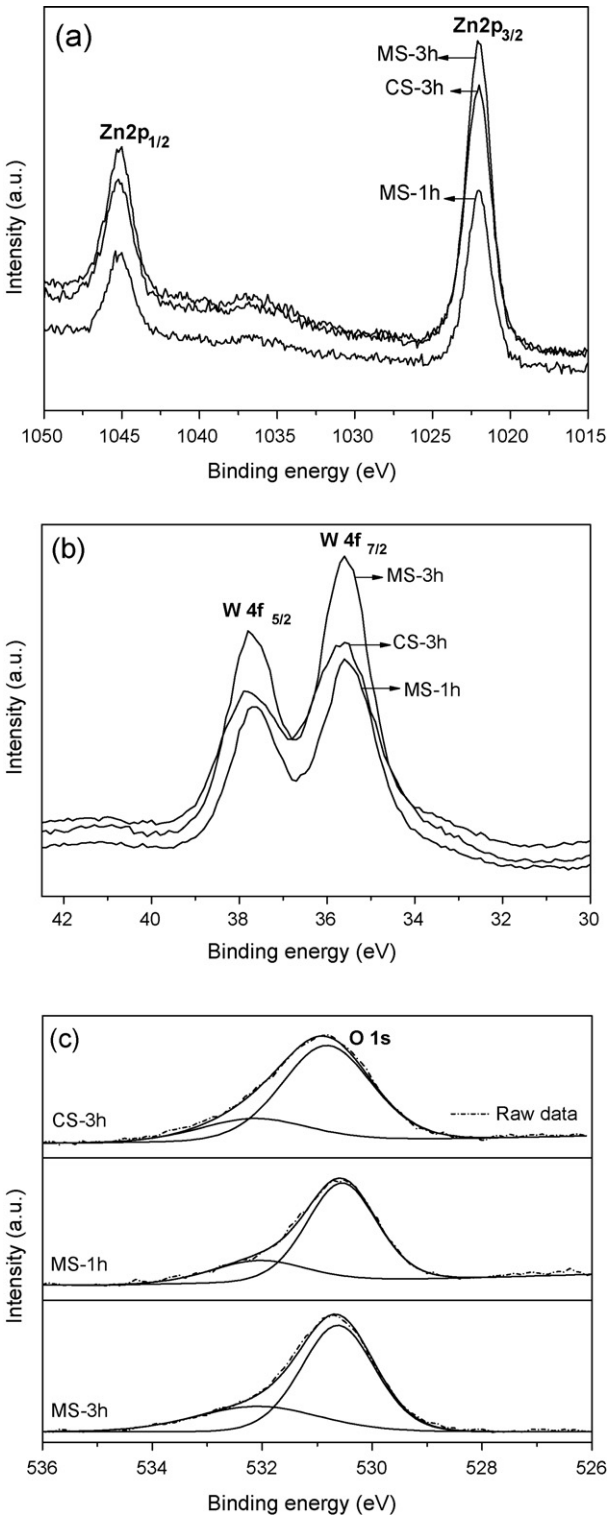

Fig. 4. High-resolution XPS spectra of nanocrystalline $ZnWO_4$: (a) Zn 2p; (b) W 4f; (c) O 1s.

X-ray photoelectron spectroscopy surface measurements were performed on $ZnWO_4$ powders to determine the elemental composition and oxidation state. Fig. 4 shows the Zn 2p, W 4f and O 1s XPS spectra for nanocrystlline $ZnWO_4$. It can be observed that these three samples show similar patterns. From Fig. 4a, the XPS peaks are sharp and symmetric, which demonstrates the existence of Zn^{2+} in

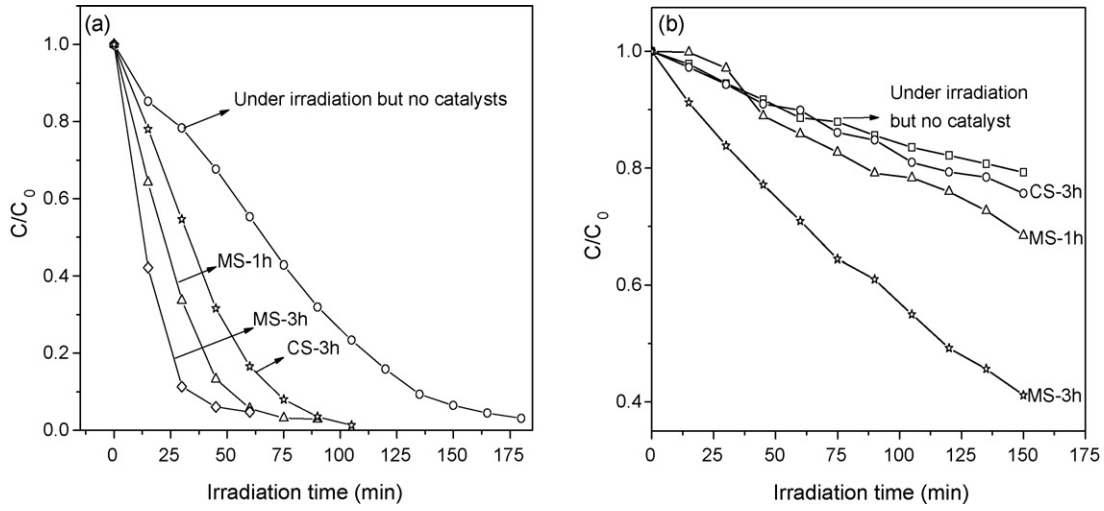

Fig. 5. Concentration changes of RhB at 554 nm and SA at 297 nm as a function of irradiation time in the presence of photocatalysts: (a) Rhodamine B and (b) salicylic acid.

the products [41]. The XPS spectra of W 4f (Fig. 4b) show a resolved doublet due to the tungsten $4f_{7/2}$ and $4f_{5/2}$ components observed at binding energies of 35.58 eV and 37.76 eV, respectively. The difference in binding energy of the resolved doublet is 2.18 eV which is in agreement with the standard value. These clearly show that the samples only contain W^{6+} state [42]. The O1s XPS spectra are shown in Fig. 4c. The asymmetry of these O1s broad bands is indicative of the presence of at least two types of oxygen species on the surface. One at about 530.6 eV or 530.8 eV was assigned to lattice oxygen ions [43] and the other at 532.1 eV was associated with the adsorbed oxygen or oxygen in the hydroxyl group [44]. The ratios of these different oxygen species (adsorbed oxygen or oxygen in the hydroxyl group:lattice oxygen ions) for sample CS-3h, MS-1h and MS-3h are 0.28, 0.3, and 0.4, respectively.

Photocatalytic activities of the samples were evaluated by the degradation of SA and RhB in the aqueous solution under UV irradiations (λ = 254 nm). Temporal changes in the concentration of SA and RhB are monitored by examining the variations in maximal absorption in UV–vis spectra at 297 nm and 554 nm, respectively. Fig. 5 exhibits the concentration changes of SA and RhB as a function of irradiation time. It can be observed that the photocatalytic activities follow the order of MS-3h > MS-1h > CS-3h for the decomposition of both SA and RhB. However the photocatalytic activities of all samples are still lower than that of P-25. The BET surface areas of the samples show very little difference, indicating the influence of surface areas on the photocatalytic activity can be neglectable in our case. From XRD analysis, it can be observed that the crystallization of the samples follows the order of MS-3h > MS-1h > CS-3h which is in agreement with the photocatalytic activity order. It has been reported that higher crystallization can usually lead to enhanced photocatalytic activity by suppressing the recombination of photogenerated holes and electrons. Meanwhile, sample MS-3h has actually more adsorbed oxygen or oxygen in the hydroxyl group, as confirmed by the XPS results. Therefore we ascribe the higher photocatalytic activity of the samples prepared by the solvothermal process to their better crystallization and larger concentration of adsorbed oxygen. In order to quantitatively understand the reaction kinetics of RhB and SA degradation in our experiments, we applied the pseudo-first order model as expressed by Eq. (1), which is generally used for photocatalytic degradation process if the initial concentration of pollutant is low [45]:

$$\ln\left(\frac{C_0}{C}\right) = kt \quad (1)$$

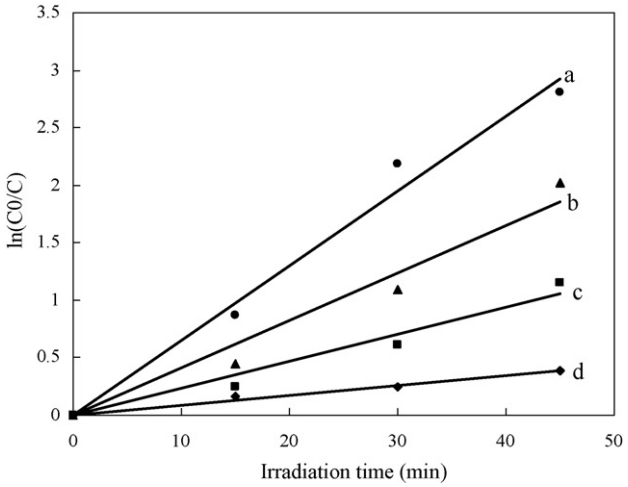

Fig. 6. Kinetics of RhB removal in solutions: (a) MS-3h; (b) MS-1h; (c) CS-3h; (d) under irradiation but no catalysts.

where C_0 and C are the concentrations of the pollutants in solution at time 0 and t, respectively, and k is the pseudo-first order rate constant. The photocatalytic reaction kinetics of RhB and SA degradation in solution based on the data plotted in Fig. 5 are presented at Figs. 6 and 7. The rate constants obtained from the

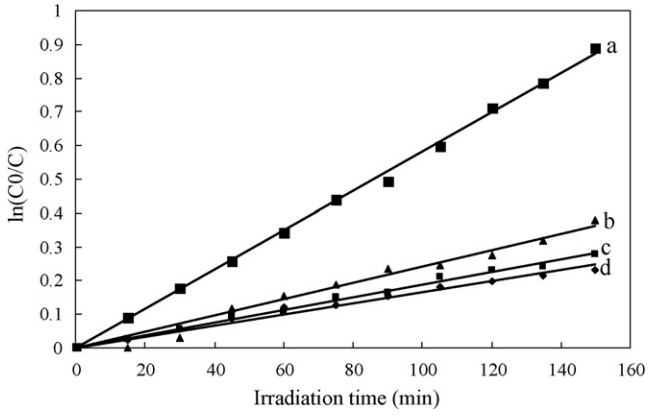

Fig. 7. Kinetics of SA removal in solutions: (a) MS-3h; (b) MS-1h; (c) CS-3h; (d) under irradiation but no catalysts.

Table 1
The pseudo-first order rate constants of SA and RhB photo-decomposition.

Sample	k_{RhB}/k_{SA}	R_{RhB}/R_{SA}
MS-3h	0.065/0.0058	0.9837/0.9982
MS-1h	0.0413/0.0024	0.965/0.975
CS-3h	0.0234/0.0019	0.9603/0.9931
Under irradiation but no catalyst	0.0087/0.0017	0.9858/0.9816

regression lines are included in Table 1. As can be observed, a fairly good correlation to the pseudo-first order reaction kinetics ($R > 0.96$) was found, indicating the reaction is pseudo-first order reaction.

4. Conclusions

$ZnWO_4$ nanoparticle is synthesized by a facile microwave-assisted solvothermal process for the first time. This method can produce $ZnWO_4$ nanoparticles in a shorter time, therefore, can save time and energy. The induced particles are about 10 nm. The sample prepared by the microwave-assisted solvothermal process for 3 h exhibits the highest photocatalytic activity for the degradation of salicylic acid and Rhodamine B because of its higher crystallinity and more adsorbed oxygen. The photocatalytic reaction is a pseudo-first order reaction via the kinetic analysis.

Acknowledgements

The author would like to thank the support of National Natural Science Foundation of China (20571015, 20777011, and 20537010), National Key Basic Research Program of China (973 Program: 2007CB613306 and 2008CB617507), and grants from Natural Science Foundation of Fujian Province (E0510011) and Scientific Project of Fujian Province (2005HZ1008), China.

References

[1] S.H. Yoon, D.W. Kim, S.Y. Cho, K.S. Hong, J. Eur. Ceram. Soc. 26 (2006) 2051.
[2] M. Daturi, G. Busca, M.M. Borel, A. Leclaire, P. Piaggio, J. Phys. Chem. B 101 (1997) 4358.
[3] T.N. Nikolaenko, Yu.A. Hizhnyi, S.G. Nedilko, J. Lumin. 128 (2008) 807–810.
[4] A. Dodd, A. McKinley, T. Tsuzuki, M. Saunders, J. Eur. Ceram. Soc. 29 (2009) 139–144.
[5] S. Lin, J.B. Chen, X.L. Weng, L.Y. Yang, X.Q. Chen, Mater. Res. Bull. (2008), doi:10.1016/j.materresbull.2008.10.011.
[6] H.B. Fu, J. Lin, L.W. Zhang, Y.F. Zhu, Appl. Catal. A: General 306 (2006) 58.
[7] X. Cao, W. Wu, N. Chen, Y. Peng, Y. Liu, Sens. Actuators B: Chem. (2008), doi:10.1016/j.snb.2008.11.020.
[8] F.G. Yang, C.Y. Tu, H.Y. Wang, Y.P. Wei, Z.Y. You, G.H. Jia, J.F. Li, Z.J. Zhu, X.A. Lu, Y. Wang, J. Alloys Compd. 455 (2008) 269–273.
[9] M. Bonanni, L. Spanhel, M. Lerch, E. Fuglein, G. Muller, Chem. Mater. 10 (1998) 304–307.
[10] J.H. Zhou, X.T. Chen, J. Li, L.H. Li, J.M. Hong, Z.L. Xue, X.Z. You, Chem. Phys. Lett. 375 (2003) 185.
[11] Y.J. Xiong, Y. Xie, Z.Q. Li, X.X. Li, S.M. Gao, Chem. -Eur. J. 10 (2004) 654.
[12] J.H. Ryu, C.S. Lim, W.C. Oh, K.B. Shim, J. Ceram. Process. Res. 5 (2004) 316.
[13] J.H. Ryu, C.S. Lim, K.H. Auh, Mater. Lett. 57 (2003) 9.
[14] G.L. Huang, C. Zhang, Y.F. Zhu, J. Alloys Compd. 432 (2007) 269–276.
[15] P. Parhi, T.N. Karthik, V. Manivannan, J. Alloys Compd. 465 (2008) 380–386.
[16] T.T. Dong, Z.H. Li, Z.X. Ding, L. Wu, X.X. Wang, X.Z. Fu, Mater. Res. Bull. 43 (2008) 1694–1701.
[17] D.M.P. Mingos, D.R. Baghurst, Chem. Soc. Rev. 20 (1991) 1.
[18] D.V. Louzguine-Luzgin, G.Q. Xie, S. Li, A. Inoue, N. Yoshikawa, K. Mashiko, S. Taniguchi, M. Sato, J. Alloys Compd. (2008), doi:10.1016/j.jallcom.2008.07.158.
[19] B.L. Newalkar, J. Olanrewaju, S. Komarneni, Chem. Mater. 13 (2001) 552.
[20] L. Perreux, A. Loupy, Tetrahedron 57 (2001) 9199.
[21] K.S. Jung, J.H. Kwon, S.M. Son, J.S. Shin, G.D. Lee, S.S. Park, Synth. Met. 141 (2004) 259.
[22] T. Thongtem, S. Kaowphong, S. Thongtm, Appl. Surf. Sci. 254 (2008) 7765–7769.
[23] L.S. Cavalcante, J.C. Sczancoski, L.F. Lima Jr., J.W.M. Espinosa, P.S. Pizani, J.A. Varela, E. Longo, Crys. Growth Des 9 (2009) 1002.
[24] L. Wu, J.H. Bi, Z.H. Li, X.X. Wang, X.Z. Fu, Catal. Today 131 (2008) 15.
[25] H. Arami, M. Mohajerani, M. Mazloumi, R. Khalifehzadeh, A. Lak, S.K. Sadrnezhaad, J. Alloys Compd. 469 (2009) 391–394.
[26] J.C. Scazacoski, L.S. Cavalcante, M.R. Joya, J.A. Varela, P.S. Pizani, E. Longo, Chem. Eng. J. 140 (2008) 632–637.
[27] X.B. Cao, C. Zhao, X.M. Lan, D. Yao, W.J. Shen, J. Alloys Compd. (2008), doi:10.1016/j.jallcom.2008.06.138.
[28] C.H. Lu, B. Bhattacharjee, S.Y. Chen, J. Alloys Compd. (2008), doi:10.1016/j.jallcom.2008.08.042.
[29] A. Kajbafvala, M.R. Shayegh, M. Mazloumi, S. Zanganeh, A. Lak, M.S. Mohajerani, S.K. Sadrnezhaad, J. Alloys Compd. 469 (2009) 293–297.
[30] M. Zawadzki, J. Alloys Compd. 454 (2008) 347–351.
[31] P. Parhi, V. Manivannan, J. Alloys Compd. (2008), doi:10.1016/j.jallcom.2008.02.010.
[32] S. Farhadi, Z. Momeni, M. Taherimehr, J. Alloys Compd. (2008), doi:10.1016/j.jallcom.2008.03.113.
[33] Z. Chen, Y.W. Yan, J.M. Liu, Y. Yin, H.M. Wen, J.Q. Zao, D.H. Liu, H.M. Tian, C.S. Zhang, S.D. Li, J. Alloys Compd. (2008), doi:10.1016/j.jallcom.2008.05.060.
[34] Y. Liu, Q. Li, G.W. Lin, K.C. Chou, K.D. Xu, J. Alloys Compd. 468 (2009) 455–461.
[35] A.C.F.M. Costa, D.A. Vieira, V.J. Silva, V.C.S. Diniz, R.H.G.A. Kiminami, L. Gama, J. Alloys Compd. (2008), doi:10.1016/j.jallcom.2008.08.096.
[36] S. Komarneni, R. Roy, Q.H. Li, Mater. Res. Bull. 27 (1992) 1393.
[37] S.F. Liu, I.R. Abothu, S. Komarneni, Mater. Lett. 38 (1999) 344.
[38] H.S. Potdar, S.B. Deshpande, A.S. Deshpande, S.P. Gokhale, S.K. Date, Y.B. Khollam, A. Patil, J. Mater. Chem. Phys. 74 (2002) 306.
[39] G. Kortum, Reflectance Spectroscopy, Springer-Verlag, New York, 1966.
[40] J.I. Pankove, Optical Process in Semiconductors, Dover, New York, 1971.
[41] H.H. Wang, C.S. Xie, Physica E 40 (2008) 2724–2729.
[42] M.A. Cortés-Jácome, C. Angeles-Chavez, E. López-Salinas, J. Navarrete, P. Toribio, J.A. Toledo, Appl. Catal. A: General 318 (2007) 178–189.
[43] C. Cantalini, H.T. Sun, M. Faccio, M. Pelino, S. Santucci, L. Lozzi, M. Passacantando, Sens. Actuators B 31 (1996) 81–87.
[44] H.B. Zou, S.Z. Chen, W.M. Lin, J. Nat. Gas Chem. 17 (2008) 208–211.
[45] J.M. Herrmann, H. Ahiri, Y. Ait-Ichou, G. Lassaletta, A.R. Gonzalez-Elipe, A. Fernandez, Appl. Catal. B 13 (1997) 219.